

This article was downloaded by:

On: 25 January 2011

Access details: *Access Details: Free Access*

Publisher *Taylor & Francis*

Informa Ltd Registered in England and Wales Registered Number: 1072954 Registered office: Mortimer House, 37-41 Mortimer Street, London W1T 3JH, UK



## Separation Science and Technology

Publication details, including instructions for authors and subscription information:

<http://www.informaworld.com/smpp/title~content=t713708471>

### The Influence of Protein Size on Adsorption Kinetics and Equilibria in Ion-Exchange Chromatography

G. Garke<sup>a</sup>; R. Hartmann<sup>a</sup>; N. Papamichael<sup>a</sup>; W. -D. Deckwer<sup>a</sup>; F. B. Anspach<sup>a</sup>

<sup>a</sup> BIOCHEMICAL ENGINEERING DIVISION, GBF-GESELLSCHAFT FÜR BIOTECHNOLOGISCHE FORSCHUNG mbH, MASCHERODER WEG 1, BRAUNSCHWEIG, GERMANY

Online publication date: 15 September 1999

**To cite this Article** Garke, G. , Hartmann, R. , Papamichael, N. , Deckwer, W. -D. and Anspach, F. B.(1999) 'The Influence of Protein Size on Adsorption Kinetics and Equilibria in Ion-Exchange Chromatography', *Separation Science and Technology*, 34: 13, 2521 — 2538

**To link to this Article:** DOI: 10.1081/SS-100100788

URL: <http://dx.doi.org/10.1081/SS-100100788>

## PLEASE SCROLL DOWN FOR ARTICLE

Full terms and conditions of use: <http://www.informaworld.com/terms-and-conditions-of-access.pdf>

This article may be used for research, teaching and private study purposes. Any substantial or systematic reproduction, re-distribution, re-selling, loan or sub-licensing, systematic supply or distribution in any form to anyone is expressly forbidden.

The publisher does not give any warranty express or implied or make any representation that the contents will be complete or accurate or up to date. The accuracy of any instructions, formulae and drug doses should be independently verified with primary sources. The publisher shall not be liable for any loss, actions, claims, proceedings, demand or costs or damages whatsoever or howsoever caused arising directly or indirectly in connection with or arising out of the use of this material.

## The Influence of Protein Size on Adsorption Kinetics and Equilibria in Ion-Exchange Chromatography

G. GARKE, R. HARTMANN, N. PAPAMICHAEL,

W.-D. DECKWER, and F. B. ANSPACH\*

BIOCHEMICAL ENGINEERING DIVISION

GBF - GESELLSCHAFT FÜR BIOTECHNOLOGISCHE FORSCHUNG mbH

MASCHERODER WEG 1, D-38124 BRAUNSCHWEIG, GERMANY

### ABSTRACT

The adsorption behavior of lysozyme and  $\gamma$ -globulin on the strong cation-exchanger Streamline SP was studied by determining the equilibrium isotherms with batch experiments. Adsorption isotherms of the binary mixture of both proteins were modeled using the Langmuir parameters derived from single-component systems. Comparison of experimental results with the competitive Langmuir model displayed significant deviations for the adsorption of lysozyme in the mixture. An extended Langmuir model, accounting for the distinct accessibility of the sorbent's surface for the competing proteins, revealed much better consistency with experimental data. Assuming the rate-limiting step of protein uptake is due to mass transport effects, the kinetics were modeled with a rate model. Taking into account diffusion across the liquid film and within the adsorbent pores, effective pore diffusion coefficients were determined. It was shown that the effective pore diffusion coefficient of both model proteins depends on the total protein concentration and the concentration ratio of the competing proteins in the liquid phase. In the binary mixture the diffusion rate of the faster diffusing protein lysozyme was slowed down by the lower diffusion rate of the larger protein  $\gamma$ -globulin. In packed bed experiments the weaker adsorbed  $\gamma$ -globulin was displaced by lysozyme and eluted earlier as in single-component breakthrough curves whereas the elution time of lysozyme was almost identical. However, the breakthrough curve of lysozyme was flatter in the presence of  $\gamma$ -globulin due to the diffusional hindrance in the mixture.

**Key Words.** Ion-exchange chromatography; Protein adsorption; Protein accessibility; Displacement effects; Discount factor; Adsorption kinetics

\* To whom correspondence should be addressed. Telephone: +49 531 6181 743. FAX: +49 531 6181 175. E-mail: Anspach@gbf.de

## INTRODUCTION

Ion exchangers are the most commonly used stationary phases for protein purification in downstream processing (1). This is attributed to their versatility and relatively low price. In order to keep operating costs low during large-scale operation, working in the nonlinear regime of protein adsorption isotherms is recommended. This results in a higher throughput of both sample volume and protein, but the associated higher bed loading leads to notable competition between proteins for binding sites at the sorbent's surface. As a consequence, displacement and, in unfavorable circumstances, a lowering of the effective binding capacity for the target protein is observed.

The optimization of chromatographic operations becomes increasingly important with scale. To describe and optimize a chromatographic purification step by computer simulation, an understanding of the equilibrium and the kinetics of adsorption is necessary. Ideally, fundamental parameters derived from batch experiments would be used within a computer model in order to plan and modify the chromatographic purification step (2, 3).

Different strategies exist for modeling preparative chromatography (4). Two fundamental approaches are mainly employed to solve the problem of distribution effects. One approach, generally termed the plate theories, simplifies the mathematical treatment by lumping various bandspreading contributions into a plate height. However, the plate height is not directly related to physicochemical parameters of proteins and hence this is a more empirical approach (5–7).

The other approach is more complex and based on differential mass balance equations. Several so-called rate models have been developed for the adsorption of proteins on porous media (2, 8, 9). Apart from the thermodynamics of phase equilibrium, the rate models consider the axial dispersion and mass transfer resistance, e.g., the external fluid film resistance,  $k_f$ , and the intra-particle effective pore diffusion coefficient,  $D_{eff}$ . Experimental validation of various chromatographic models for protein adsorption has usually addressed single-component systems (7, 10, 11) or a mixture of small organic molecules (12). The complexity increases with systems consisting of more than one component, as an increasing number of coefficients must be determined independently by measurement. The problem of how many and which parameters are substantial for a successful description of a real chromatographic separation, e.g., a fermentation broth supernatant, is still to be solved.

In order to get insight into the effects during adsorption of a protein mixture, a two-component system with well-defined boundary conditions was chosen. Lysozyme and  $\gamma$ -globulin were used as model proteins with the strong cation-exchanger Streamline SP in a batch system. A film and pore diffusion model based on a Langmuir-type adsorption was employed to describe the



mass transport for the two-component system. The issues of protein competition and different accessibilities of the ion-exchanger's inner surface were addressed and related to the breakthrough behavior of binary mixtures of different lysozyme/γ-globulin ratios.

## THEORETICAL ASPECTS

### Equilibria

Assuming reversible second-order kinetics for the adsorption of proteins, equilibria can be described by the well-known Langmuir isotherm (13). Although this model was proposed for the adsorption of gases on surfaces, it is well suited to describe protein adsorption if single-site interactions take place between the protein and the ligand and if additional nonspecific interactions are absent. To describe mixed gas adsorption, Markham (14) employed the competitive Langmuir equation

$$q_i^* = \frac{q_m K_{ai} c_i^*}{1 + \sum_j K_{aj} c_j^*} \quad (1)$$

in which  $q_m$  represents the maximum binding capacity,  $q_i^*$  and  $c_i^*$  the sorbate concentration in the solid and liquid phases at equilibrium, and  $K_{ai}$  the association constant of Component  $i$ .

The binding capacities of two proteins can be similar when they are related to the sorbent's surface area; nevertheless, they can differ when related to the volume of the sorbent. This is the case if pore size exclusion effects come into play due to different sizes of these proteins. A discount factor,  $\delta$ , defined as the ratio of  $q_{m1}$  to  $q_{m2}$ , was introduced to take into account distinct saturation capacities  $q_{mi}$ , caused by different accessibilities of the ion-exchange surface for proteins of different sizes and shapes (15). In a two-component system, competition for a particular site is only relevant if both proteins have physical access to that site. If Protein 1 is larger than Protein 2, only a fraction of adsorption sites for Protein 2 are available to Protein 1, which is expressed as  $0 < \delta = q_{m1}/q_{m2} \leq 1$ . The second-order differential kinetics for Component 1 are then described by Eq. (2). It should be pointed out that  $\delta$  is not related to the ratio of the particle porosity,  $\epsilon_p$ , for each of the proteins, as the contribution of small pores to the binding capacity of a sorbent is relatively higher than that of large pores.

$$dq_1/dt = k_{a1}c_1 (q_{m1} - q_1 - \delta q_2) - k_{d1}q_1 \quad (2)$$

The rate constants of adsorption and desorption are represented by  $k_a$  and  $k_d$ . From the second-order differential kinetics for Components 1 and 2, Eqs. (3)



and (4) are derived for the equilibrium concentration  $q_1^*$  and  $q_2^*$  (15), with  $K_{ai} = k_{ai}/k_{di} = 1/K_{di}$ .

$$q_1^* = \frac{K_{a1}c_1^*[(1 + K_{a2}c_2^*)q_{m1} - \delta K_{a2}c_2^* q_{m2}]}{1 + K_{a1}c_1^* + K_{a2}c_2^* + (1 - \delta)K_{a1}c_1^*K_{a2}c_2^*} \quad (3)$$

$$q_2^* = \frac{K_{a2}c_2^*[(1 + K_{a1}c_1^*)q_{m2} - K_{a1}c_1^* q_{m1}]}{1 + K_{a1}c_1^* + K_{a2}c_2^* + (1 - \delta)K_{a1}c_1^*K_{a2}c_2^*} \quad (4)$$

When  $q_{m1} = q_{m2}$  ( $\delta = 1$ ), Eqs. (3) and (4) reduce to the common two-component Langmuir equation derived from Eq. (1). Equations (3) and (4) may be solved algebraically (16) using the Langmuir parameters  $K_{ai}$  and  $q_{mi}$  determined from single-component measurements.

## Kinetics

To determine the effective pore diffusion coefficients via uptake curves, a heterogeneous film and pore diffusion model was employed. It was derived from the differential mass balance (see Eq. 5) with the particle porosity for each of the proteins,  $\varepsilon_p$ , the concentration  $c_p$  in the pore volume, the effective pore diffusion coefficient  $D_{eff}$ , and the particle radius  $r$  (from 0 to  $R_p$ , the average particle radius). Particle porosities  $\varepsilon_p$  were determined from size exclusion experiments in the packed bed mode under nonbinding conditions (1 M NaCl). For lysozyme and  $\gamma$ -globulin, 0.7 and 0.36 were obtained, respectively.

$D_{eff}$  is smaller than the diffusivity  $D_0$  in solution as a result of two effects: the random orientation of the pores, which gives a longer diffusion path, and the variation of pore diameters. Both effects are commonly accounted for by a tortuosity factor  $\tau$ :  $D_{eff} = D_0\varepsilon_p/\tau$ . To describe the protein distribution between the pore liquid and the particle surface, the second-order kinetic (2) was used, assuming that the rate of the adsorption is not a limiting step.

$$\varepsilon_p \frac{\partial c_p}{\partial t} = \varepsilon_p D_{eff} \left( \frac{\partial^2 c_p}{\partial r^2} + \frac{2\partial c_p}{r\partial r} \right) - (1 - \varepsilon_p) \frac{\partial q}{\partial t} \quad (5)$$

The external film mass transfer coefficient  $k_f$  may be achieved according to an empirical equation of Geankoplis (17). The rate of mass transfer through the external film relates the bulk liquid concentration  $c_b$  to the pore liquid at the surface of the particle at the right-hand boundary in a linear form:

$$\varepsilon_p D_{eff} \frac{\partial c_p}{\partial r} = k_f(c_b - c_p), \quad r = R_p \quad (6)$$

The decrease of liquid concentration in the bulk volume is calculated from the mass balance of applied and adsorbed amount of proteins. Therefore, it is



necessary to integrate over the particle radius  $r$  (Eq. 7). The second integral, the amount of protein in the pore volume, can be neglected. This is reasonable because the amount of protein in the pore volume is small compared to the adsorbed protein and that in the bulk volume. If the capacity  $q$  is related to the whole particle volume, the factor  $(1 - \varepsilon_p)$  in the first integral is not needed.

$$\varepsilon[c_0 - c_b(t)] = \frac{3(1 - \varepsilon)(1 - \varepsilon_p)}{R_p^3} \int_0^{R_p} q(r)r^2 dr + \frac{3(1 - \varepsilon)\varepsilon_p}{R_p^3} \int_0^{R_p} c_p(r)r^2 dr \quad (7)$$

In Eq. (7),  $\varepsilon$  is the sorbent void volume fraction related to the bath. The set of equations were solved numerically for the initial and boundary conditions (9) via a FORTRAN program.

## MATERIALS AND METHODS

### Materials

The strong cation-exchanger Streamline SP (Pharmacia Biotech, Uppsala; Sweden) was used throughout this study. The macroporous matrix is based on 6% crosslinked agarose with sulfopropyl moieties and a particle size distribution between 100 and 300  $\mu\text{m}$ . The density of the moist gel varies between 1.15 and 1.20  $\text{g}\cdot\text{mL}^{-1}$ , according to the manufacturer.

Porcine  $\gamma$ -globulin (156 kDa, pI = 6.5, from Cohn fraction II, III) and lysozyme from chicken egg white (14.1 kDa, pI = 11) were purchased from Sigma (Deisenhofen, Germany). Buffer salts and reagents were obtained from Riedel-de Haen (Seelze, Germany).

### Preparation of Protein Solutions

100 mM sodium acetate buffer (pH 5) was filtered through a 0.2- $\mu\text{m}$  cellulose nitrate filter (Minisart NML, Sartorius, Germany) before use. Protein solutions were prepared by adding acetate buffer to the protein samples and stirring slowly for 30 minutes. Lysozyme solutions were clear whereas those of  $\gamma$ -globulin were cloudy. A clear solution was obtained after filtration through a paper filter (Wei $\beta$ band, Schleicher & Sch $\ddot{\text{u}}$ ll, Dassel, Germany). Mixtures of the two proteins were prepared by combination and dilution. Individual protein concentrations of mixtures were determined by HPLC analysis.

### Batch Adsorption

After equilibration of the ion-exchanger with 100 mM acetate buffer (pH 5), 0.3 g samples of moist gel were weighed into 5 mL test tubes. Different vo-



lumes of protein solution were added and the tubes gently rotated for 2 hours at 25°C. After allowing the gel to settle (1 minute), the quantity of adsorbed protein per mL gel was determined by calculation of the loss of protein in the supernatant. This value was corrected for the protein present in the pore volume and related to the settled volume of the ion exchanger.

### Protein Uptake Curves

An amount (0.3 g) of the ion-exchange gel was washed, equilibrated, and weighed into 5 mL test tubes. A defined volume with known protein concentration was added, and the tube was rotated a predefined time period,  $t$ . After the gel settled (1 minute), the adsorbed protein was calculated from the remaining protein concentration in the liquid phase. A series of 10 tests was performed under identical conditions with contact times varying between 1 and 100 minutes.

### Analysis of the Two-Component Protein Mixture by Size Exclusion Chromatography

Protein mixtures were separated by size exclusion chromatography (HPLC system 2150-52, LKB, Bromma, Sweden; Superose 12 column, 310  $\times$  10 mm, Pharmacia Biotech, Uppsala, Sweden), using 50 mM potassium phosphate buffer with 150 mM NaCl (pH 7.0) at a flow rate of 0.75 mL·min $^{-1}$ . Proteins were detected at 280 nm using a calibrated UV-detector.

### Frontal Analysis

The adsorption behavior of the two proteins was observed in packed-bed experiments as breakthrough curves. The column experiments were performed with 13 mL Streamline SP packed in a XK-16 column (diameter 16 mm, bed height 65 mm) and an FPLC system (Pharmacia Biotech, Uppsala, Sweden). In all experiments the volumetric flow rate was 0.83 mL·min $^{-1}$  (linear flow rate 25 cm·h $^{-1}$ ). After equilibration with 100 mM sodium acetate buffer (pH 5), the column was loaded with protein solution until the concentration at the outlet reached that of the inlet. The compositions of the effluents were analyzed by HPLC, as described above. After adsorption, bound proteins were eluted with a linear gradient up to 1 M NaCl and the Streamline sorbent was regenerated with 0.5 M NaOH + 1.5 M NaCl.

## RESULTS AND DISCUSSION

### Single-Component Adsorption

According to the theory outlined above, the description of the competitive binding and displacement phenomena requires a knowledge of the individual



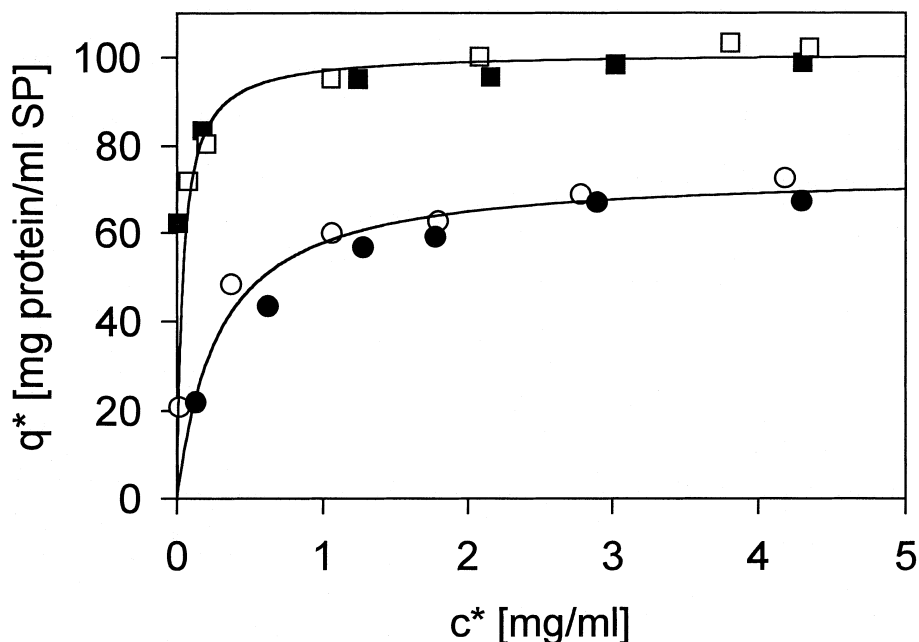


FIG. 1 Adsorption isotherms of lysozyme (■, □) and  $\gamma$ -globulin (●, ○) on Streamline SP in 100 mM sodium acetate buffer (pH 5). Two independent series of adsorption experiments were performed for each protein. The lines are obtained from least-square fitting of the Langmuir model. Corresponding Langmuir parameters are listed in Table 1.

protein adsorption isotherms. Isotherms for lysozyme and  $\gamma$ -globulin are shown in Fig. 1. The Langmuir parameters were calculated by least-squares regression of Scatchard-plot data and are summarized in Table 1. Adsorption of  $\gamma$ -globulin is characterized by a lower maximum capacity than lysozyme. The shallower curvature of the  $\gamma$ -globulin isotherm also indicates a lower affinity of sorbent and protein. The affinity in ion-exchange adsorption is related to the net charge of the protein and the ion exchanger. Since the pI of  $\gamma$ -

TABLE 1  
Langmuir Parameters of Single-Component Adsorption of Lysozyme and  $\gamma$ -Globulin on Streamline SP in 100 mM Acetate Buffer (pH 5)

Protein	$K_d$ (mg·mL <sup>-1</sup> )	$K_a$ (mL·mol <sup>-1</sup> )	$q_m$	
			mg·mL <sup>-1</sup>	mmol·mL <sup>-1</sup>
Lysozyme	0.041	$3.4 \times 10^5$	101	$7.2 \times 10^{-3}$
$\gamma$ -Globulin	0.280	$5.6 \times 10^5$	74	$0.47 \times 10^{-3}$



globulin is much lower than that of lysozyme, its net positive charge is relatively low at the chosen pH.

The curves clearly support the notion of a protein monolayer during binding. In contrast to this, isotherms determined under different experimental conditions, e.g., at neutral pH, were evidently at odds with a Langmuir supposition. For example, data obtained with  $\gamma$ -globulin on the anion-exchanger Streamline DEAE at pH 7.0 displayed S-type adsorption (data not shown), indicating buildup of a multilayer. Similar observations were obtained for murine IgG<sub>1</sub> on the anion-exchanger DEAE-Sepharose CL-6B (18). In the case of BSA adsorption on Streamline SP at pH 5, the curvature of the isotherm was best described using the Freundlich formalism (19). These facts illustrate how restricted the concept of a model protein is. Not only does the choice of model protein/sorbent have a distinct effect on isotherm shape, the conditions at which the adsorption takes place can also be of significant influence.

### Two-Component Adsorption

Adsorption isotherms of the binary mixture of  $\gamma$ -globulin and lysozyme are shown in Figs. 2 and 3, respectively. The solid lines depict the predictions

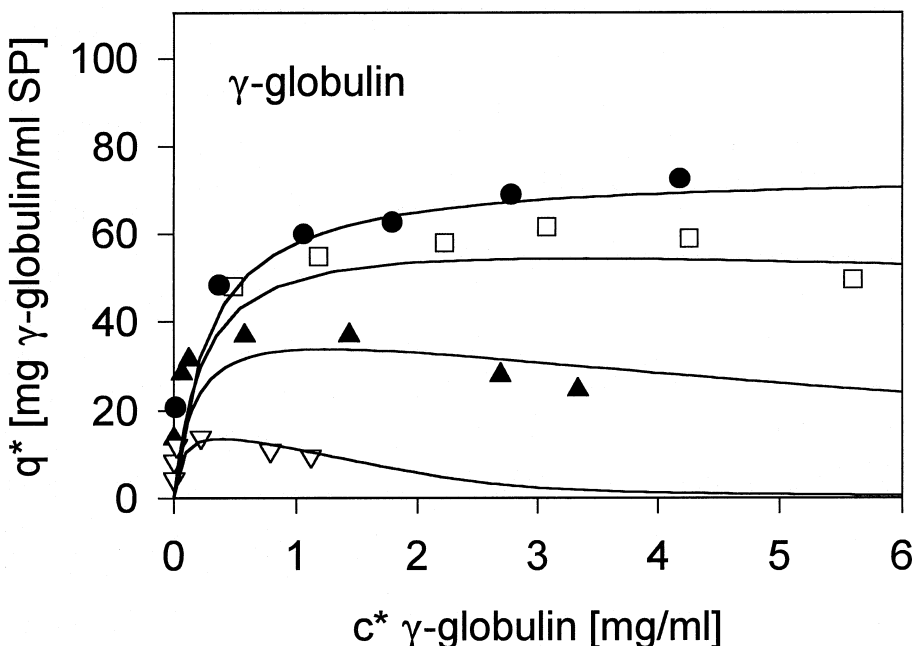


FIG. 2 Adsorption isotherms of  $\gamma$ -globulin from the binary mixture containing lysozyme;  $\bullet$  = 100%,  $\square$  = 80%,  $\blacktriangle$  = 50%, and  $\triangledown$  = 20% mass fraction of  $\gamma$ -globulin in  $c^0$ . Solid lines are calculated using the full-competitive two-component Langmuir Eq. (1), utilizing parameters derived from experiments with individual proteins (Table 1).



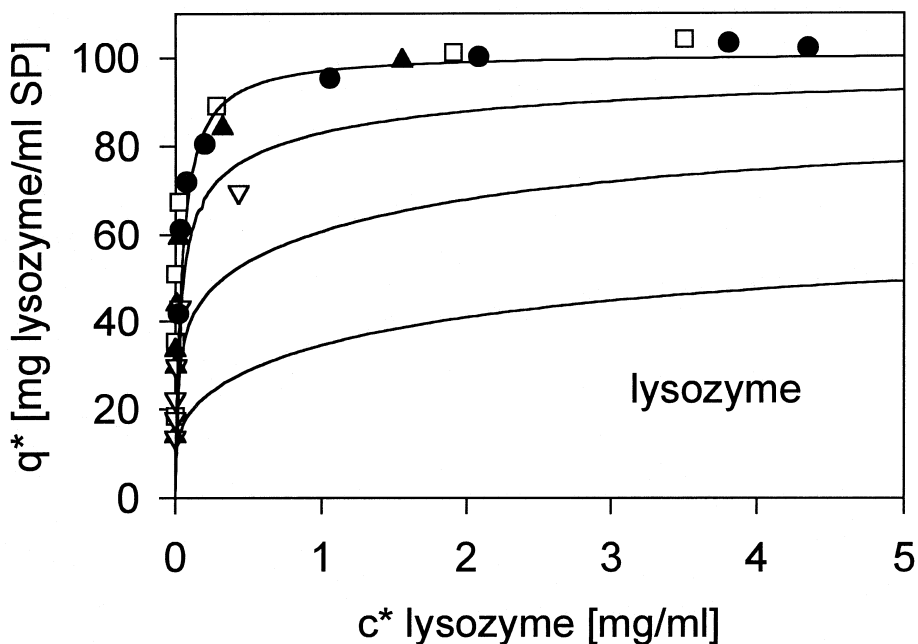


FIG. 3 Adsorption isotherms of lysozyme from the binary mixture containing  $\gamma$ -globulin;  $\bullet$  = 100%,  $\square$  = 80%,  $\blacktriangle$  = 50%, and  $\nabla$  = 20% mass fraction of lysozyme in  $c^0$ . Solid lines are calculated using the full-competitive two-component Langmuir Eq. (1), utilizing Langmuir parameters derived from experiments with individual proteins (Table 1).

from the full-competitive Langmuir model described by Eq. (1). The mass fractions of the two proteins refer to the conditions at  $c^0$  (at start of protein adsorption from the mixture), which were set to 1.0, 0.8, 0.5, and 0.2 for  $\gamma$ -globulin; these protein compositions change during adsorption until equilibrium is reached.

The adsorption isotherm of  $\gamma$ -globulin in the binary mixture shows competitive behavior. Competition between the two proteins for free binding sites resulted in a displacement effect which was observed as a decreasing  $\gamma$ -globulin binding capacity with increasing total protein concentration in the feedstock. The maximum capacity for  $\gamma$ -globulin, as obtained either from the asymptotic values or from the maxima of the curves in Fig. 2, was found to be proportional to the mass fraction in  $c^0$ , as is shown in Fig. 4. Hence, the competitive Langmuir model was well-suited to describe the adsorption of  $\gamma$ -globulin from the binary protein mixture.

In contrast to this, adsorption isotherms of lysozyme in the binary mixture were found to be similar to those of the pure protein with the maximum binding capacity not decreasing with the mass fraction of  $\gamma$ -globulin in  $c^0$ . In other words, the adsorption behavior of lysozyme is almost independent of the second component,  $\gamma$ -globulin. The full-competitive model predicts a de-



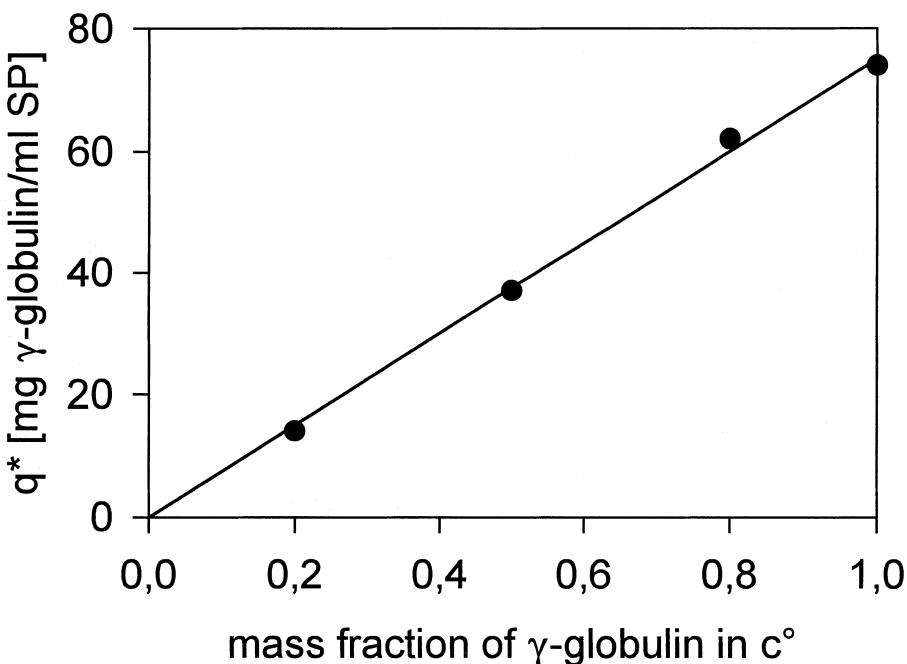


FIG. 4 Dependence of the maximum binding capacity of  $\gamma$ -globulin on the mass fraction in  $c^0$  of the binary mixture containing lysozyme.

crease of the binding capacity with increasing the  $\gamma$ -globulin mass fraction which, however, was not observed in practice. A possible explanation for this contradiction may be derived by considering the shapes of the two proteins. Figure 5 shows schematically the molecular dimensions of lysozyme, a globular protein (20), and  $\gamma$ -globulin, an ellipsoid (21). Due to the size of  $\gamma$ -globulin, only a small portion of the surface area is accessible, the rest being only

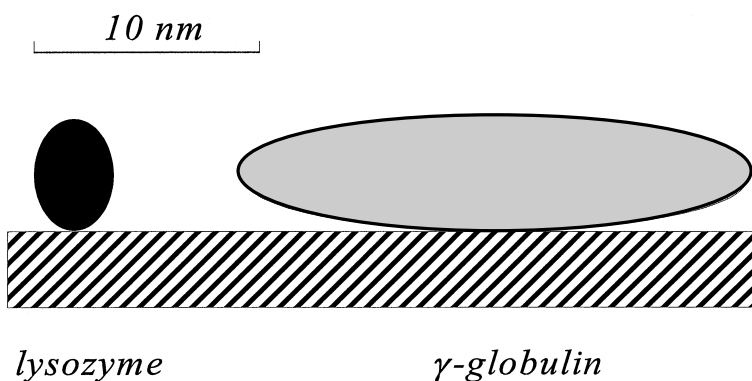


FIG. 5 Scheme of the molecular dimensions of lysozyme and  $\gamma$ -globulin.



accessible to the smaller molecule lysozyme. Hence, competition between  $\gamma$ -globulin and lysozyme for binding sites takes place only within the fully accessible fraction. Competition effects at those sites may be only marginal in comparison to the total binding capacity for lysozyme. Therefore, the large deviation found between predicted and experimental data of the full-competitive adsorption model is due to the assumption that the same surface is reachable for both proteins which, however, is unreal.

Mathematically, this situation is accounted for by the extended multicomponent Langmuir model of Eqs. (3) and (4) (15). Accordingly, the factor  $\delta$  was set to the ratio of the maximum binding capacities for single-component adsorption  $\delta = q_{m1}/q_{m2} = 0.73$ . The results are shown in Fig. 6 for lysozyme. In contrast to the full-competitive isotherm model, the restricted access model properly predicts the adsorption isotherms for both  $\gamma$ -globulin and lysozyme from the binary mixture. For  $\gamma$ -globulin there is only a marginal change in the predicted behavior compared to the original predictions in Fig. 2. For lysozyme this model offers much better agreement between experimental data and simulated curves than the full-competitive Langmuir model. In essence, the  $\delta$ -factor allows a more comprehensive description of the competition between lysozyme and  $\gamma$ -globulin. Corresponding to these results, the maximum

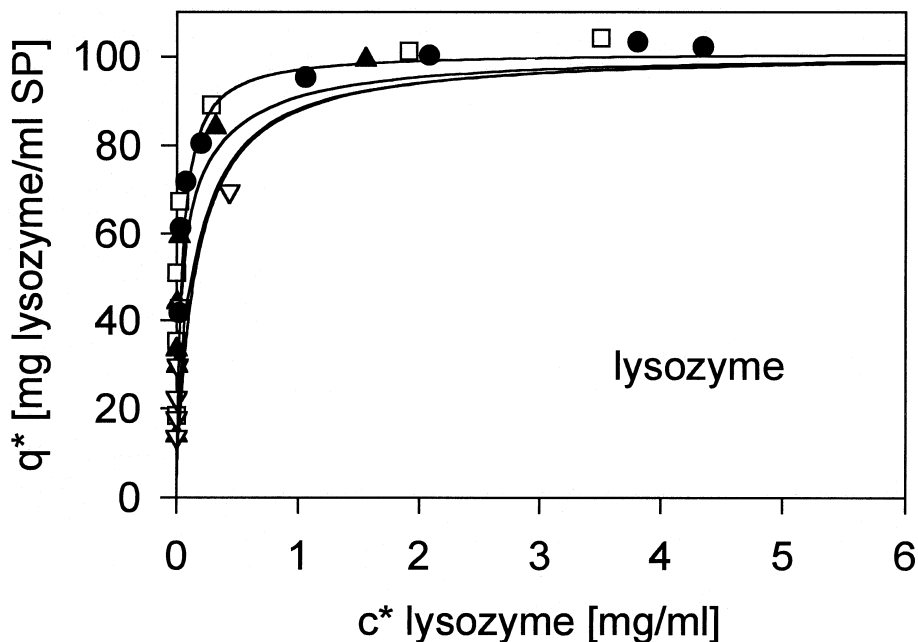


FIG. 6 Adsorption isotherms of lysozyme from the binary mixture containing  $\gamma$ -globulin;  $\bullet = 100\%$ ,  $\square = 80\%$ ,  $\blacktriangle = 50\%$ , and  $\nabla = 20\%$  mass fraction of lysozyme in  $c^0$ . Same experimental data of binary mixture as in Fig. 3. Solid lines were calculated utilizing the extended two-component Langmuir Eqs. (3) and (4) with  $\delta = q_{m1}/q_{m2} = 0.73$ ; lines for 20% and 50% mass fraction of lysozyme are not resolved in the graph.



binding capacity for lysozyme is only marginally affected by  $\gamma$ -globulin. Therefore, besides the thermodynamic constants  $K_{ai}$  and  $q_{mi}$  the accessible pore fraction of competing proteins is an important factor to consider in order to predict the binding capacities of individual proteins from a binary mixture.

### Adsorption Kinetics

Experimental protein uptake curves were determined and compared to simulated curves by varying the effective pore diffusion coefficient,  $D_{\text{eff}}$ , in the pore and film diffusion model. Optimization at simulated curves was done by least-squares regression until the best fit was obtained. The particles were assumed to be monodisperse with a radius of 100  $\mu\text{m}$  (mean value from a distribution of 50–150  $\mu\text{m}$ ), and the film mass transfer coefficients,  $k_f$ , were estimated according to Geankoplis (17) to be  $9.1 \times 10^{-6}$  and  $4.4 \times 10^{-6} \text{ m} \cdot \text{s}^{-1}$  for lysozyme and  $\gamma$ -globulin, respectively. Normalized concentrations,  $c/c^0$ , were plotted against the square root of the contact time,  $t$ , which is the sum of the mixing and settling times. Figures 7 and 8 (solid lines) show the uptake curves for single-component adsorption of  $\gamma$ -globulin and lysozyme at initial concentrations,  $c^0$ , of 8 and 4  $\text{g} \cdot \text{L}^{-1}$ , respectively. In the initial period of ad-

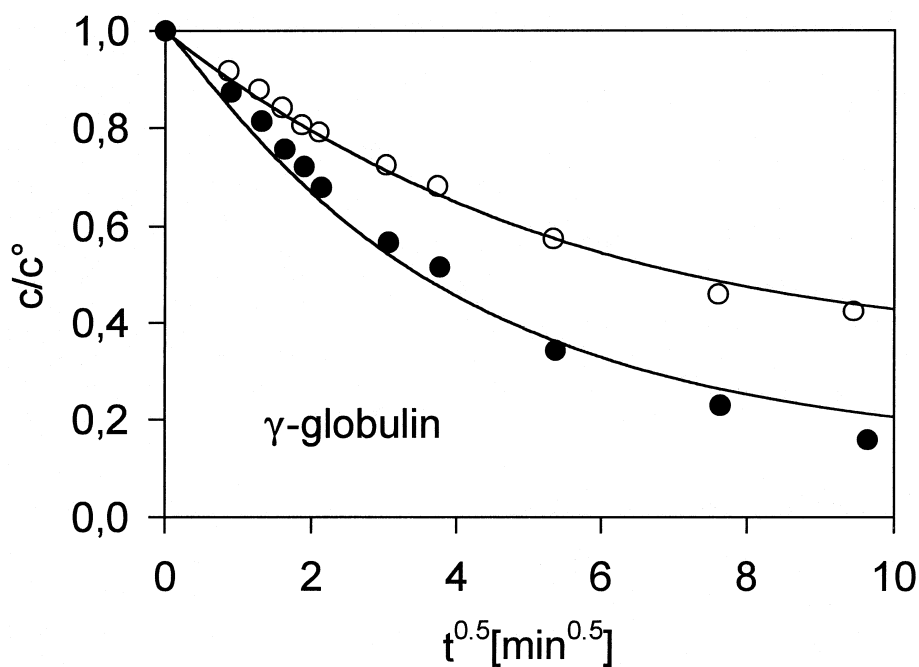


FIG. 7 Batch adsorption profiles of the uptake of  $\gamma$ -globulin by Streamline SP in agitated vessels. The concentrations at the start were 4 and 8  $\text{g} \cdot \text{L}^{-1}$ . Solid lines were calculated with the film and pore diffusion model. The adsorption of  $\gamma$ -globulin (5 mL solution) by 0.4 g Streamline SP,  $k_f = 4.40 \times 10^{-6} \text{ m} \cdot \text{s}^{-1}$ ; ( $\bullet$ )  $c^0 = 4 \text{ g} \cdot \text{L}^{-1}$  and  $D_{\text{eff}} = 1.5 \times 10^{-11} \text{ m}^2 \cdot \text{s}^{-1}$ , ( $\circ$ )  $c^0 = 8 \text{ g} \cdot \text{L}^{-1}$  and  $D_{\text{eff}} = 0.86 \times 10^{-11} \text{ m}^2 \cdot \text{s}^{-1}$ .



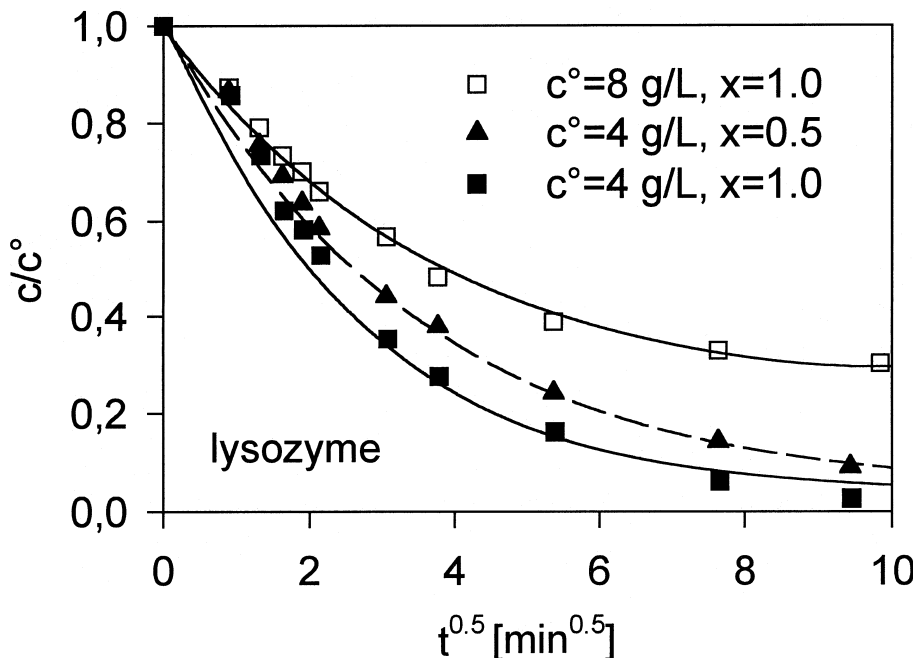


FIG. 8 Batch adsorption profiles of single- and two-component uptake of lysozyme by Streamline SP in agitated vessels. The starting concentrations were 4 and  $8 \text{ g} \cdot \text{L}^{-1}$  with mass fraction,  $x$ , of 1.0. In the binary mixture with  $\gamma$ -globulin the starting concentration was  $4 \text{ g} \cdot \text{L}^{-1}$  with a mass fraction,  $x$ , of 0.5. The adsorption of lysozyme (5 mL solution) by 0.3 g Streamline SP,  $k_f = 9.11 \times 10^{-6} \text{ m} \cdot \text{s}^{-1}$ ; ( $\blacksquare$ )  $c^0 = 4 \text{ g} \cdot \text{L}^{-1}$ ,  $x = 1.0$ , and  $D_{\text{eff}} = 2.2 \times 10^{-11} \text{ m}^2 \cdot \text{s}^{-1}$ ; ( $\square$ )  $c^0 = 8 \text{ g} \cdot \text{L}^{-1}$ ,  $x = 1.0$ , and  $D_{\text{eff}} = 1.4 \times 10^{-11} \text{ m}^2 \cdot \text{s}^{-1}$ ; ( $\blacktriangle$ )  $c^0 = 4 \text{ g} \cdot \text{L}^{-1}$ ,  $x = 0.5$ , and  $D_{\text{eff}} = 1.4 \times 10^{-11} \text{ m}^2 \cdot \text{s}^{-1}$ .

sorption the film and pore diffusion model predicts a faster decrease of the bulk concentration than determined experimentally. This discrepancy is most probably due to the experimental setup. The diameter of the stagnant film around a particle is a function of the relative motion of the liquid to the particle. Hence, it is smaller during mixing than during the time the ion-exchange particles are allowed to settle. Since the settling time was invariably 1 minute, the effect of the larger mass transfer resistance was more pronounced at the beginning of uptake, especially during the first 5 minutes. Variation of the film mass transport coefficient had only a minor impact on the shape of the curve with advancing adsorption time, demonstrating that mass transport inside the porous system is rate limiting. Although a better fit at the onset of the protein uptake curve could be attained by variation of  $k_f$ , this was disregarded due to the known variation of the film thickness as consequence of the experimental setup (see above).

The results indicate that mass transfer within the pores is concentration-dependent, the diffusivity being faster at an initial concentration of  $4 \text{ g} \cdot \text{L}^{-1}$  than at  $8 \text{ g} \cdot \text{L}^{-1}$ . The higher protein concentration probably leads to increased steric



interactions between the molecules themselves and between molecules and the pore walls of the sorbent, which results in hindered diffusion.

Comparison of the uptake curves for lysozyme at a concentration of  $4 \text{ g}\cdot\text{L}^{-1}$  in the absence and presence of  $\gamma$ -globulin demonstrates the influence of the latter component (Fig. 8). Lysozyme uptake in the binary mixture (broken line) is obviously retarded when  $\gamma$ -globulin is present.

Using the computer simulation program for single-component adsorption and optimizing  $D_{\text{eff}}$  by least-squares fit, the uptake curve for the two-component system was modeled. This approach can only be justified for the case of lysozyme, the adsorption of which is relatively independent of the presence of  $\gamma$ -globulin. Table 2 summarizes the effective diffusion coefficients for both the single- and two-component systems. There are two trends: first,  $D_{\text{eff}}$  is concentration-dependent for both proteins, decreasing with increasing concentration; second, the effective pore diffusivity of lysozyme in the binary system decreases with the mass fraction of the competing  $\gamma$ -globulin. It appears that the presence of  $\gamma$ -globulin effectively masks the rise expected at the lower lysozyme concentration. In other words, the hindrance caused by the competitor molecule becomes an overriding factor, so much so that the effective diffusivity of lysozyme approaches the value for  $\gamma$ -globulin as the mixture becomes richer in the latter.

Similar phenomena were observed during investigation of the pore diffusion of organic dyes in activated carbon (22). It was found that  $D_{\text{eff}}$  of the single-component solutions varied with  $c^0$  with an exponential decay function. From measurements of the diffusion rates in multisolute systems, the effective diffusion coefficient of the slower molecule was found to be enhanced and that

TABLE 2  
Effective Pore Diffusion Coefficients of Lysozyme and  $\gamma$ -Globulin during Adsorption from Pure Solution and from Two-Component Mixtures, as Calculated with the Film and Pore Diffusion Model

Initial concentration, $c^0 \text{ (g}\cdot\text{L}^{-1}$		$D_{\text{eff}} \times 10^{11} \text{ (m}^2\cdot\text{s}^{-1})^a$	
$\gamma$ -Globulin	Lysozyme	$\gamma$ -Globulin	Lysozyme
0	4.0	—	2.2
0	8.0	—	1.4
1.3	6.7	—	2.0
4.0	4.0	—	1.4
6.5	1.5	—	1.0
4.0	0	1.5	—
8.0	0	0.9	—

<sup>a</sup> In free solution:  $D_{\text{bulk}} (\gamma\text{-globulin}) = 4.0 \times 10^{-11} \text{ m}^2\cdot\text{s}^{-1}$ ,  $D_{\text{bulk}} (\text{lysozyme}) = 11.2 \times 10^{-11} \text{ m}^2\cdot\text{s}^{-1}$  (28, 23).



of the faster diffusing molecule reduced. Whether a similar effect would be observed for  $\gamma$ -globulin can only be ascertained by extending the current computer program and obtaining values for its effective diffusivity in the protein mixture.

Assuming the protein diffusion coefficient in solution is independent of concentration, which, however, is only realistic at dilute concentrations (23), an additional transport mechanism must be taken into consideration in order to account for the observed effects. It has been suggested that surface diffusion participates in the mass transfer of proteins, especially at high protein concentrations of ion exchangers of high charge density (24). Nevertheless, in order to account for the diffusional interference in the mixture of both proteins, numeric coupling via cross coefficients in the mathematical description (25) must be allowed.

### Breakthrough Curves

The consequences of displacement effects in the binary mixture on breakthrough curves in comparison to single-component systems are shown in Fig. 9. Due to the lack of a kinetic model to account for two-component adsorption on an ion exchanger, the simulation of breakthrough curves is yet to come.

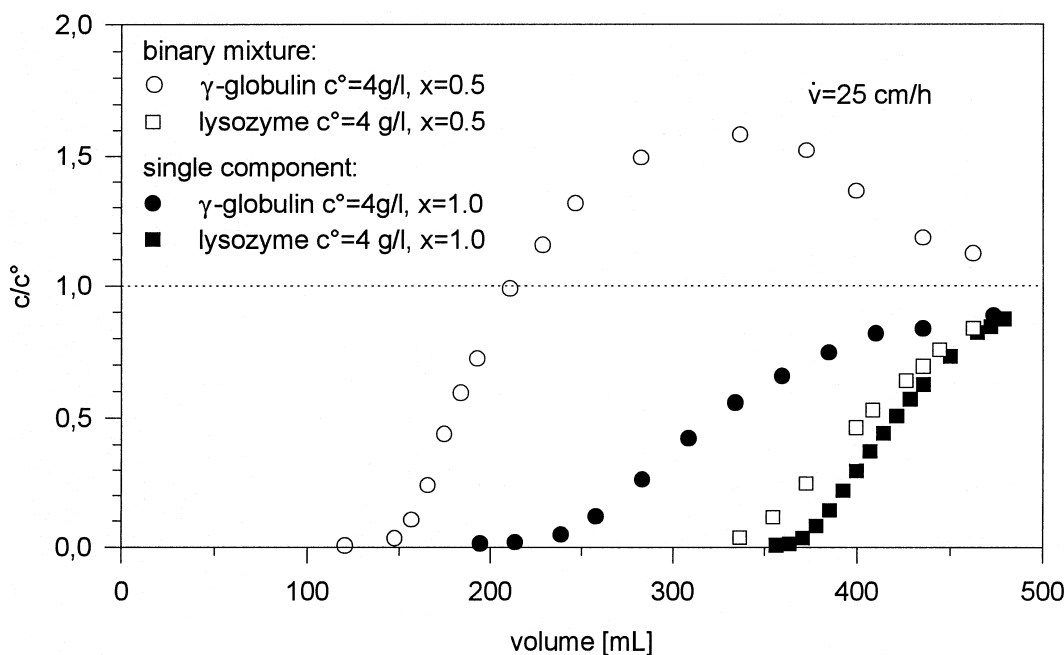


FIG. 9 Breakthrough curves of  $\gamma$ -globulin and lysozyme in single-component solutions and binary mixtures. The initial concentration of each protein was  $4 \text{ g} \cdot \text{L}^{-1}$  with different mass fractions,  $x$ , of 1.0 and 0.5. The volumetric flow rate was  $0.83 \text{ mL} \cdot \text{min}^{-1}$  with a column diameter of 16 mm and a bed volume of 13 mL Streamline SP in 100 mM acetate buffer (pH 5).



In the single-component experiments the breakthrough of  $\gamma$ -globulin occurs earlier and the slope of the curve is shallower than that of lysozyme. These observations can be easily explained by considering the isotherm and findings from protein uptake experiments. Both the binding capacity,  $q_m$ , for  $\gamma$ -globulin and its effective pore diffusion coefficient,  $D_{eff}$ , are lower compared to lysozyme. Hence, penetration into the particle will be slower, allowing the protein to be washed out by convective flow at an earlier stage. The shallow curvature reflects the fact that  $\gamma$ -globulin exhibits a lower degree of diffusive penetration.

Furthermore, the curve for  $\gamma$ -globulin does not reach the level of the inlet concentration, even after 500 mL have passed through the column. The slower effective diffusivity at higher protein concentration might play a role here, but another interpretation is that this behavior is related to replacement effects, which are inherently dependent on the desorption kinetics (26). A similar explanation has been previously termed the "parking" problem by Jin et al. (27) and is described by the random sequential adsorption (RSA) algorithm. Essentially, at high surface coverage proteins need a long time to find free adsorption sites before they can "park" themselves, as cars have to do in a parking lot. At low coverage, sites are available almost everywhere, so that the time required to park is significantly lower. The present model assumes that the rate-limiting step is dependent only on mass transfer effects. Hence, such statistically driven adsorption behavior cannot be described accurately.

The breakthrough curve determination for the binary mixture exhibits a "roll-up" phenomenon in the case of  $\gamma$ -globulin, reaching a concentration at a maximum of approximately 1.6-fold of the entry value. In addition, the curve is steeper and appears earlier in comparison to the pure protein loading. The curve for lysozyme, in contrast, is marginally flatter but essentially retains its original shape and position. From the batch adsorption isotherms it was evident that lysozyme displaces  $\gamma$ -globulin. Initially, there is binding of both proteins. As sites are utilized, competition becomes more relevant and  $\gamma$ -globulin is displaced by lysozyme. Hence, the effective volume for binding of  $\gamma$ -globulin is reduced dynamically and an earlier breakthrough occurs.

The breakthrough curve of lysozyme in the mixture is flatter than in the single-component experiment based on the kinetic effect described above. The diffusivity of lysozyme is slowed down in the presence of  $\gamma$ -globulin.

In the case of  $\gamma$ -globulin the capacity decreased from  $76 \text{ mg} \cdot \text{mL}^{-1}$  in the single-component breakthrough curve to  $18 \text{ mg} \cdot \text{mL}^{-1}$  in the protein mixture. For lysozyme the capacities were almost identical ( $101$  and  $100 \text{ mg} \cdot \text{mL}^{-1}$  for the single component and the mixture, respectively). Only the displaced component is eluted from  $160$  to  $330 \text{ mL}$ , and hence can be separated from the binary mixture. The capacities of the single-component breakthrough curves correlated with the findings from the single batch adsorption isotherms at  $c^*$



$= 4 \text{ mg} \cdot \text{mL}^{-1}$  (see Fig. 1). In contrast, the capacities of the binary mixture in packed-bed experiments did not correlate in the same manner with the batch isotherms. In breakthrough curve experiments there is a continual introduction of new material with constant mass fraction of the proteins. Hence, a distinct behavior can be expected with respect to capacity in these two adsorption modes. The utilization of thermodynamic data from batch isotherms in column adsorption can only be successful if this can be taken into account.

## CONCLUSION

The binding of a binary mixture of lysozyme and  $\gamma$ -globulin onto Streamline SP cannot be correctly described without consideration of the respective pore fraction accessibility for each of the proteins. Moreover, it was found that binding capacity alterations depend strongly on the relative molecular size and apparent association constant with the cation exchanger; a small competitor protein with a high net-positive charge and consequently high affinity dramatically decreasing the capacity for the larger protein with a low net-positive charge. Observations also indicate that the effective protein diffusivity was altered due to intermolecular hindrance as shown by measurements with various protein mass fractions. All these phenomena increase the complexity of a model required to describe the binding of proteins to ion-exchange sorbents adequately.

## REFERENCES

1. E. Boschetti, "Advanced Sorbents for Preparative Protein Separation Purposes," *J. Chromatogr. A*, 658, 207 (1994).
2. B. H. Arve and A. I. Liapis, "Modeling and Analysis of Biospecific Adsorption in a Finite Bath," *AIChE J.*, 33, 179 (1987).
3. I. S. Gosling, "The Design of Adsorption in Downstream Processing: The Importance of Data from Small-Scale Experiments," in *Biochemical Engineering*, (H. Chmiel, W. P. Hammes, and J. E. Bailey, Eds.), G. Fischer, New York, NY, 1987, pp. 396-401.
4. T. Gu, G.-J. Tsai, and G. T. Tsao, "Modeling of Nonlinear Multicomponent Chromatography," *Adv. Biochem. Eng. Biotechnol.*, 49, 45 (1993).
5. H. Pedersen, L. Furler, K. Venkatsubramanian, J. Prenolsil, and E. Stuker, "Enzyme Adsorption in Porous Supports: Local Thermodynamic Equilibrium Model," *Biotechnol. Bioeng.* 27, 961 (1985).
6. A. Velayudhan and M. R. Ladisch, "Plate Models in Chromatography: Analysis and Implications for Scale-Up," *Adv. Biochem. Eng. Biotechnol.*, 49, 123 (1993).
7. S. Golshan-Shirazi and G. Guiochon, "Modeling of Preparative Liquid Chromatography," *J. Chromatogr. A*, 658, 149 (1994).
8. B. H. Arve and A. I. Liapis, "Biospecific Adsorption in Fixed and Periodic Countercurrent Beds," *Biotechnol. Bioeng.*, 32, 616 (1988).
9. G. L. Skidmore, B. J. Horstmann, and H. A. Chase, "Modeling Single-Component Protein Adsorption to the Cation-Exchanger S Sepharose FF," *J. Chromatogr.*, 498, 113 (1990).



10. G. Leaver, J. A. Howell, and J. R. Conder, "Adsorption Kinetics of Albumin on a Cross-Linked Cellulose Chromatographic Ion-Exchanger," *Ibid.*, 590, 101 (1992).
11. W. A. C. Somers, A. J. J. Smolders, W. A. Beverloo, H. J. Rozie, J. Visser, F. M. Rombouts, and K. van't Riet, "Modeling the Adsorption of *endo*-Polygalacturonase on Alginate Beads," *Bioseparation*, 4, 285 (1994).
12. W. Zihao and Z. Kefeng, "Kinetics and Mass Transfer for Lactic Acid Recovered with Anion Exchange Method in Fermentation Solution," *Biotechnol. Bioeng.*, 47, 1 (1995).
13. I. Langmuir, "The Constitution and Fundamental Properties of Solids and Liquids," *J. Am. Chem. Soc.*, 38, 2221 (1916).
14. E. C. Markham and A. F. Benton, "The Adsorption of Gas Mixtures by Silica," *Ibid.*, 53, 497 (1931).
15. T. Gu, G.-J. Tsai, and G. T. Tsao, "Multicomponent Adsorption and Chromatography with Uneven Saturation Capacities," *AIChE J.*, 37, 1333 (1991).
16. A. O. Converse and D. J. Girard, "Effect of Substrate Concentration on Multicomponent Adsorption," *Biotechnol. Prog.*, 8, 587 (1992).
17. C. J. Geankoplis, *Transport Processes and Unit Operations* 2nd ed., Allyn and Bacon, Boston, MA, 1983.
18. F. B. Anspach, D. Petsch, and W.-D. Deckwer, "Purification of Murine IgG1 on Group Specific Affinity Sorbents," *Bioseparation*, 6, 165 (1996).
19. H. Freundlich, "Über die Adsorption in Lösungen," *Z. Phys. Chem.*, 57, 385 (1906).
20. S. Tsuneda, H. Shinano, K. Saito, S. Furusaki, and T. Sugo, "Binding of Lysozym onto a Cation-Exchange Microporous Membrane Containing Tentacle-Type Grafted Polymer Branches," *Biotechnol. Prog.*, 10, 76 (1994).
21. R. F. Schmidt and G. Thews, *Physiologie des Menschen*, 19th ed., Springer Verlag, Berlin, 1977, p. 321.
22. B. Al-Duri and G. McKay, "Pore Diffusion: Dependence of the Effective Diffusivity on the Initial Sorbate Concentration in Single and Multisolute Batch Adsorption Systems," *J. Chem. Tech. Biotechnol.*, 55, 245 (1992).
23. M.-T. Tyn, and T. W. Gusek, "Prediction of Diffusion Coefficients of Proteins," *Biotechnol. Bioeng.*, 35, 327 (1990).
24. H. Yoshida, M. Yoshikawa, and T. Kataoka, "Parallel Transport of BSA by Surface and Pore Diffusion in Strongly Basic Chitosan," *AIChE J.*, 40, 2034 (1994).
25. W. Merk, W. Fritz, and E. U. Schlünder, "Competitive Adsorption of Two Dissolved Organics onto Activated Carbon—III," *Chem. Eng. Sci.*, 36, 743 (1980).
26. F. B. Anspach, A. Johnston, H.-J. Wirth, K. K. Unger, and M. T. W. Hearn, "High-Performance Liquid Chromatography of Amino Acids, Peptides and Proteins. XCV. Thermodynamic and Kinetic Investigations on Rigid and Soft Affinity Gels with Varying Particle and Pore Sizes: Comparison of Thermodynamic Parameters and the Adsorption Behavior of Proteins Evaluated from Bath and Frontal Analysis Experiments," *J. Chromatogr.*, 499, 103 (1990).
27. X. Jin, J. Talbot, and N.-H. L. Wang, "Analysis of Steric Hindrance Effects on Adsorption Kinetics and Equilibria," *AIChE J.*, 40, 1685 (1994).
28. C. B. Fuh, S. Levin, and J. C. Giddings, "Rapid Diffusion Coefficient Measurements Using Analytical SPLITT Fractionation: Application to Proteins," *Anal. Biochem.*, 208, 80 (1993).

Received by editor September 25, 1998

Revision received February 1999



## **Request Permission or Order Reprints Instantly!**

Interested in copying and sharing this article? In most cases, U.S. Copyright Law requires that you get permission from the article's rightsholder before using copyrighted content.

All information and materials found in this article, including but not limited to text, trademarks, patents, logos, graphics and images (the "Materials"), are the copyrighted works and other forms of intellectual property of Marcel Dekker, Inc., or its licensors. All rights not expressly granted are reserved.

Get permission to lawfully reproduce and distribute the Materials or order reprints quickly and painlessly. Simply click on the "Request Permission/Reprints Here" link below and follow the instructions. Visit the [U.S. Copyright Office](#) for information on Fair Use limitations of U.S. copyright law. Please refer to The Association of American Publishers' (AAP) website for guidelines on [Fair Use in the Classroom](#).

The Materials are for your personal use only and cannot be reformatted, reposted, resold or distributed by electronic means or otherwise without permission from Marcel Dekker, Inc. Marcel Dekker, Inc. grants you the limited right to display the Materials only on your personal computer or personal wireless device, and to copy and download single copies of such Materials provided that any copyright, trademark or other notice appearing on such Materials is also retained by, displayed, copied or downloaded as part of the Materials and is not removed or obscured, and provided you do not edit, modify, alter or enhance the Materials. Please refer to our [Website User Agreement](#) for more details.

**Order now!**

Reprints of this article can also be ordered at  
<http://www.dekker.com/servlet/product/DOI/101081SS100100788>